

Progress in the Design Process Automation for Sailing Yachts

Copyright © Ulrich Remmlinger, Germany, 2012

Abstract. The paper describes an optimization program to determine the design parameters of a sailing yacht for given constraints and merit function. The simulation program is organized in 3 layers. The outer layer is a genetic optimization of the design parameters. An intermediate layer uses a hill climbing method to determine the optimal trim parameters like apparent wind angle, sail area and sail lift coefficient distribution that yield the optimal VMG. The innermost layer calculates the equilibrium of forces (resistance, side force, sinkage) and moments (heel, pitch) by numerical root finding in 5 dimensions.

NOMENCLATURE

B_{WL}	Beam of waterline	m_K	Mass of fin keel (ballast)
C	Local chord length of foil	m_{Rig}	Mass of rig and sails
C_{KR}	Keel section root chord length	P	Mainsail max. hoist above boom
C_{KT}	Keel section tip chord length	R_{added}	Added resistance due to waves
C_P	Prismatic coefficient	R_{ind}	Induced resistance
c_{fric}	Shear drag coefficient canoe body	$R_{visc,C}$	Viscous resistance, canoe body
c_L	Lift coefficient of foil section	$R_{visc,K}$	Viscous resistance, keel
c_{tot}	Total drag coefficient canoe body	$R_{wave,C}$	Wave making resistance, canoe body
c_{visc}	Viscous drag coefficient canoe body	$R_{wave,K}$	Wave making resistance, keel
D_C	Depth canoe body from keel root to roof	S	Distance sail head to water pl. along mast
E	Mainsail max. foot length	T	Maximum draft including keel
$F_{par,rig}$	Parasitic drag force, rig	T_C	Draft of canoe body
$F_{par,hull}$	Parasitic drag force, hull	t_{KR}	Keel section root thickness
I	Fore triangle max. hoist above deck	t_{KT}	Keel section tip thickness
J	Foot length of fore triangle	∇	Volume displacement of hull and fin keel
LCB	Dist. longitude. centre of buoyancy to fpp	α	Flare angle at midship section
L_{OA}	Length overall	β	Deadrise angle at midship section
L_{WL}	Length of waterline	γ	local dimensionless circulation
m_c	Mass of hull (canoe body)	ρ_w	Density of water

1. INTRODUCTION

The design of a sailing yacht is an iterative process, commonly known as the design spiral. Even with the use of modern CAD-systems and Velocity Prediction Programs (VPP) these iteration loops are often terminated before the desired optimum is reached. Especially for cruising yachts the additional time and funding for the design work are not available. In this circumstance an automation of the design process would be desirable.

For blue water cruising yachtmen the performance in two critical operating points distinguishes a good design. When tacking in very light winds and when tacking under gale conditions, in both cases it is essential to make good progress to windward. On all other courses and in medium winds the yacht's performance is usually sufficient. For a fast passage in a predictable time it is therefore necessary to optimize the yacht for these critical conditions. In consequence a merit function will be defined as a weighted average of the "Velocity Made Good" (VMG) at two different wind speeds. If desired, the computer program can also use other mixes for the merit function. For racing yacht design the elapsed time on a given course (e.g. triangle) should and can be used.

2. GEOMETRIC REPRESENTATION OF THE YACHT

The definition of the hull form starts with the midship section that is composed of a spline curve below the waterline and of an arc above the waterline. The other sections are affine transformations of the midship section. This keeps the form mathematically simple and reduces computing time when the intersection with the heeled water plane needs to be computed. The spline coefficients and the transformation are chosen in such a way that the design parameters L_{OA} , L_{WL} , B_{WL} , T_C , D_C , C_P , LCB , ∇ and β are matched. To demonstrate how this works the design parameters of the YD-40 in [1] are used for the transformation to resemble the YD-40 as closely as possible. The result is shown in figure 1. The agreement of the underwater part of the hull with the lines drawing in [1] is sufficient. Additional parameters T , C_{KR} , C_{KT} , t_{KR} and t_{KT} describe the fin keel. The sailplan is defined by the IOR rig dimensions I , J , E and P .

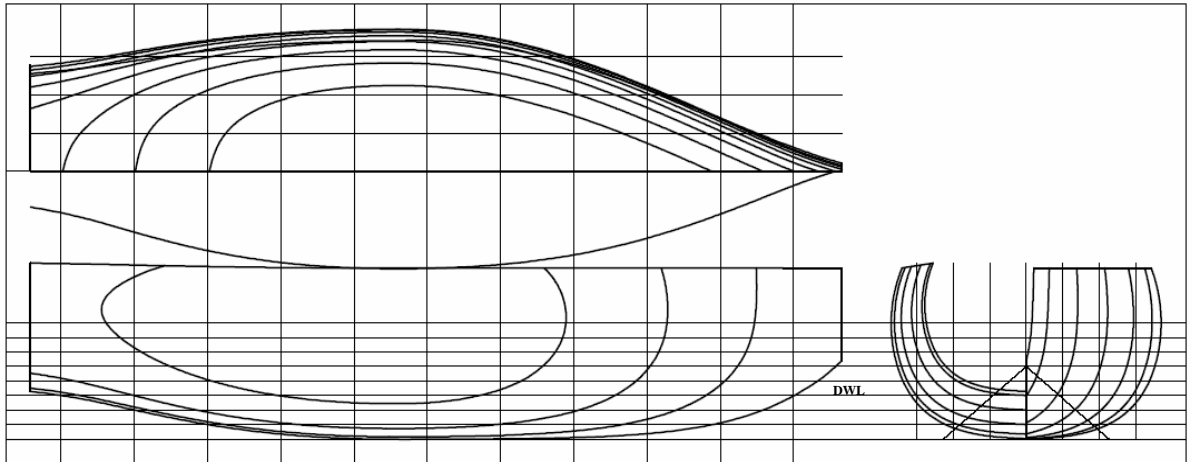


Figure 1. Mathematically simple hull form to match YD-40 design parameters

Not all mathematically possible combinations of design parameters yield a meaningful design. If a spline with an unrealistic curvature of the midship section is needed to match the given ∇ , the design is discarded.

A weight calculation must check the balance of weight and buoyancy. An estimate for the mass of the hull can be derived from the scantling rules given in [2]. The ballast mass must be iteratively determined from

$$m_K = \nabla \cdot \rho_W - m_C - m_{Rig} - payload \quad (1)$$

If m_K is unrealistic or negative the design is discarded. The weight of rig and sails is calculated from recommendations given in [1]. It depends on the maximal heeling force, which is taken from a stability calculation for the yacht at rest, subject to a gust of given wind speed with unreefed sails.

It is the task of the proposed computer program to optimize the design parameters in regard to the merit function. The result of the optimization will be a set of design parameters that allows the computation of the midship section, the affine transformation of the sections fore and aft and the definition of the keel and the sail plan. Together this will be the description of the optimal yacht geometry.

3. VELOCITY PREDICTION PROGRAM

The kernel of any performance optimizer is a VPP that calculates ship speed, sinkage, heel, leeway and trim angle by solving the three force equations for resistance, side force and vertical force and the two momentum equations for heel and pitch. It is common practice to calculate the total forces as the sum of the individual components that are contributed by hull, keel and sails. The absolute accuracy is not of prime importance since the purpose of the program is to calculate the difference in performance between competing designs. It is more important that the influences of the individual components are modeled in the right relation and the performance trends caused by changes in the parameters are accurately predicted.

3.1 Calculation of hydrodynamic side force

The side force of the keel is equivalent to the lift of an airplane wing. The calculation follows the scheme that is proposed in [3]. The side force of the canoe body is considered to be mainly induced by the side force of the keel. Only for hulls with sharp V-sections in the fore body a side force created by the canoe body alone based on R.T. Jones slender wing theory is added. The forces on the rudder are calculated with the Michlet software [4] and also interpolated from test results in [5].

3.2 Calculation of viscous and wave resistance of the hull

By far the most comprehensive database for predicting resistance components of sailing yachts is the matrix of tank test results of the Delft Systematic Yacht Hull Series (DSYHS). An analysis of the data was published in 1998 [6] and again in 2008 [7]. Within both methods the calculation of the frictional resistance uses the ITTC-57 friction coefficient multiplied with the dynamic head and wetted surface. Subtracting this from the total upright

resistance yields a term called residuary resistance which combines wave making resistance and form drag of the hull. The residuary resistance is then correlated to the design parameters of the hull based on a regression analysis of measurements of the DSYHS. In the 1998 version this term can become negative for low Froude numbers (< 0.15), e.g. for the models no. 1, 44 and 329, which indicates that the ITTC friction coefficient is too high. This will lead to erroneous results for the forces at full scale, since viscous drag and wave drag are scaled differently. In the 2008 version the issue is disguised, since the published table shows no values below $F_n = 0.15$. It is not surprising, that the ITTC-57 correlation line does not give good results for yacht like bodies, since it was developed for merchant marine vessels with long parallel sides that do not exist in yachts. The following approach overcomes this difficulty. The DSYHS coefficients are used to calculate the residuary resistance at model scale. The addition of the frictional term based on the ITTC coefficient yields the total resistance at model scale. Now a method described in [8] is employed for a three-dimensional boundary layer calculation of the viscous resistance at model scale. The hull is approximated by half a body of revolution of identical sectional areas and the differential equation for the boundary layer is solved by a second order Runge-Kutta scheme. If this resistance value is subtracted from the total resistance, the wave making drag at model scale remains. This wave drag can now be scaled to full size based on the identical Froude number. A second boundary layer calculation at full size will give the correct viscous resistance. The total resistance of the hull is then the sum of the wave drag and the three-dimensional viscous drag at full size. Figure 2 compares calculated drag-coefficients to test data from the towing tank. The difference between the viscous drag resulting from the boundary-layer calculation and the frictional drag according to the Delft-method is obvious. At the model scale 1/2 the Delft-method leads already to false total drag values especially at low Froude numbers. The discrepancy increases at full scale.

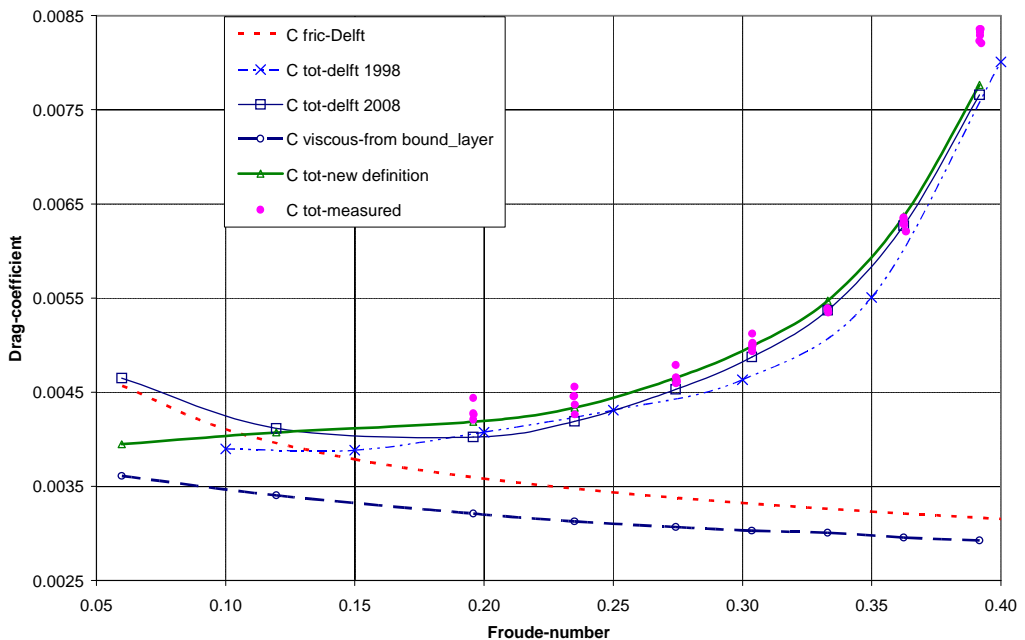


Figure 2. Resistance-coefficients of a Dehler 33 at model scale 1/2

3.2 Calculation of other resistance components

The viscous and the induced resistance of the appendages are calculated from wing theory as described in [9] and [3]. The wave making drag of the keel has been an open issue. The validity of the equations proposed in [6] is justifiably questioned in [10]. The wave making resistance of the appendages decreases as the depth of submergence increases. For a foil of small thickness and a Froude number > 0.4 based on chord, thin ship theory is applicable and the Michlet software [4] is suited to compute the wave resistance. The dependence of the resistance on the depth of submergence for an isolated foil is depicted in figure 3. As can be seen the resistance decreases very rapidly and is negligible when the submergence is larger than 30% of the chord. One can therefore assume that the wave resistance of the keel in relation to the wave resistance of the canoe body is less than the relation of the keel volume to the volume of the canoe body. For the average yacht this relation amounts to approx. 3%, so the error in the determination of the wave resistance of the keel is negligible. The much larger

values given in [6] are obviously viscous interference drag and corrections to the ITTC friction coefficient, which is not valid for hydrofoils. These corrections are subject to Reynolds- and not to Froude-scaling.

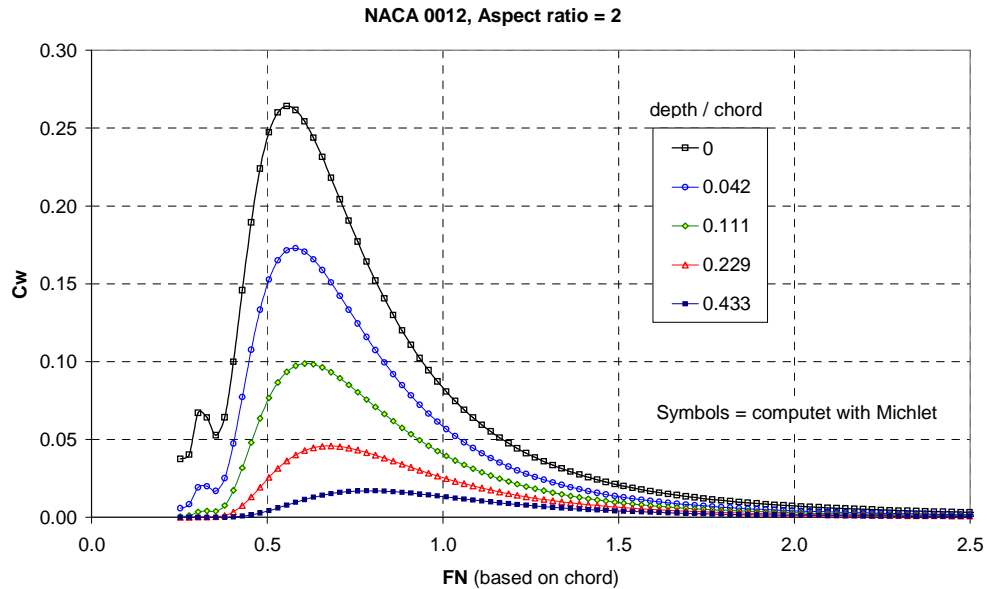


Figure 3. Wave resistance coefficient of an isolated vertical hydrofoil

The Delft-method also introduces additional resistance components due to heel and trim. We determine here the parameters that are used in the equation for the wave drag of the hull (e.g. wetted surface, L_{WL} , B_{WL} , C_P , LCB , LCF) from the hull geometry in the heeled and trimmed position. An additional term for the resistance due to heel and trim is therefore not necessary. This will improve the resistance results for hull forms where the submerged part changes drastically when heeled. The hydrostatic calculation in the correct attitude of the hull that includes an estimate for the wave profile along the hull gives the right dynamic value of the metacentric height.

The added resistance due to waves is calculated according to the polynomials in [6]. The wave height and wave period that are the input to the approximation are estimated from expressions in [11]. Fetch is varied between 200 nm at 4 kts wind speed and 50 nm at 44 kts wind speed.

3.3 Calculation of sail forces

The optimizer chooses the plan form, reefed if necessary, and creates a circulation γ distributed along the span. The span S is taken as the distance from the water plane to the sail head along the mast and divided into 30 lifting line elements. The local lift coefficient is calculated from the dimensionless local circulation according to:

$$c_L = 2 \cdot \frac{S}{C} \cdot \gamma \quad (2)$$

The local profile drag is a function of the local lift coefficient and is estimated from the polar curves in [12] that are based on water tunnel measurements. The induced drag can be calculated from the lift distribution along the lifting line, the mirror image principle is used [13]. Summing up the elements along the lifting line yields the total lift and drag coefficients and the height of the centre of effort. The lift and drag forces can then directly be calculated from the apparent wind speed at the centre of effort and the total force coefficients. This approach avoids the introduction of a sheeting angle or sail camber. It is left to the sail maker to design a sail that achieves the prescribed lift distribution for the given apparent wind angle and sail plan. The use of penalty functions in the code avoids the outcome of unrealistic lift coefficients that can not be realized by the sail maker.

3.4 Calculation of parasitic drag

Experimental results for the parasitic drag of rig, hull and superstructure are published in [14]. The difference in wind speed depending on the height above ground that is caused by the atmospheric boundary layer must be considered. For the range of interest the "law of the wall" of boundary layer theory is applicable. The wind

gradient depends on the surface roughness that can be calculated from wave height and wave period [15]. The wind speed very close to the surface varies in the wave trough compared to the wave crest [16]. Measurements can be found in [17]. The Program evaluates the parasitic drag in the trough and on the crest and uses the mean value.

An additional lift force on the hull that acts upward along the mast is reported in [14] and included in the VPP. It seems plausible that the increased wind speed over the hull creates a negative static pressure.

3.5 Solving for equilibria

After the definition of the individual force components we can now specify 5 equations for the 5 equilibria:

longitudinal forces:	driving force – resistance
side forces:	sail force – keel/hull force
vertical forces:	sail downward force – buoyancy
heeling moment:	heeling moment from side force – righting moment from keel and buoyancy
pitching moment:	pitching moment from sail force – longitudinal righting moment from buoyancy

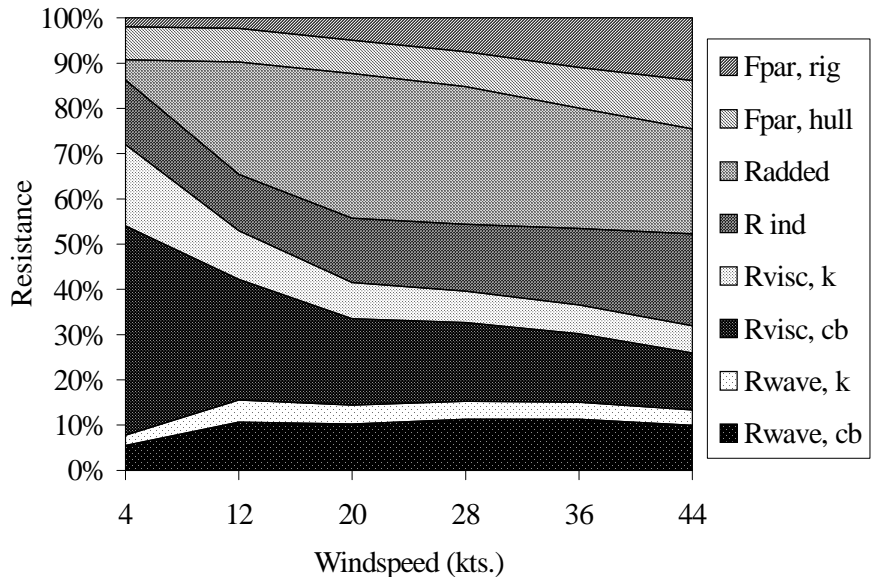
The remaining equation for the yaw momentum is not used since balance is achieved by the rudder control through the helmsman. The 5 equations allow the determination of the 5 variables: boat speed, leeway angle, heel angle, pitch angle and sinkage. This nonlinear system of equations is solved numerically [18].

4. OPTIMAL BOAT TRIM

After the solution of the equilibrium equations there is still a set of undetermined parameters. This is the distribution of the sail lift coefficients (that is based on the circulation along the lifting line), the sail area and the true wind angle. According to Glauert [13], the circulation can be approximated by a Fourier-polynomial. In this program only the first 4 terms are used. These 6 trim parameters are determined so as to maximize the speed made good to windward (VMG). A hill climbing algorithm is used for this type of optimization in multi-dimensions [18].

Figure 4 illustrates the contribution of the different resistance components at optimal trim as a function of wind speed. The YD-40 design is used as a test case [1]. At low wind speeds the drag is mainly viscous. At high wind speeds the induced drag of the keel increases because of the increased leeway angle. The parasitic drag of the rig becomes large due to the exposed part of the mast.

Figure 4. Resistance components for YD-40



The added resistance seems to play a lesser role at high wind speeds which is related to its dependence on wave height squared. At wind speeds above 30 knots the wave height increases less than linearly with wind speed and since most resistance components increase proportional to the wind speed squared the relative magnitude of the added resistance is reduced.

Figure 5 shows the optimal sail plan and the distribution of the circulation along the mast at 12 knots wind speed for the same yacht. The optimizer has created a realistic curve without areas of negative lift.

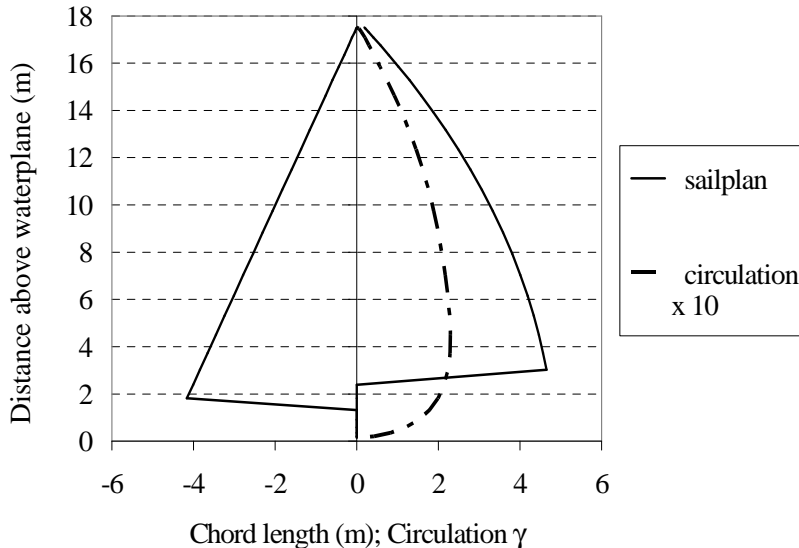


Figure 5. Circulation for YD-40 at 12 kts. wind speed

5. OPTIMAL GEOMETRY

5.1 Genetic optimization

The calculation routine described in the previous chapters determines the VMG of the yacht if it is optimally sailed and trimmed. This is preliminary work to the original task of finding the optimal geometry of hull, keel and sailplan. The use of genetic algorithms for sailing yacht optimization was introduced in [19] and is described in detail in [20]. Genetic optimization has the advantage that the result of the search is a number of good designs that are all close to the optimum but might differ substantially in the parameter sets. The designer / owner can then use personal preference to select the final design. In contrast an optimization method that uses a hill climbing strategy will only give one parameter set for the optimum. In addition the optimum of the geometric parameters is rather flat and the curve is not smooth. Hill climbing would terminate at one of the local maxima.

5.3 Constraint

Optimizing the design parameters listed in section 2 will lead to an infinite size of the yacht if no constraint is imposed on size. Several constraints were tested during the development of the program. If no class rule with maximal rating exists, which is the case for normal cruising yachts, a reasonable constraint is cost. The cost of the yacht is estimated from the structural weight as determined in chapter 2 and for rig, engine and other installations from a regression analysis of existing components on the market. Again not the absolute accuracy of the estimate is of interest, instead the cost numbers for competing designs must be in the right proportion. Alternatively it was tested to prescribe the floor space in the cabin as a constraint, but this resulted in very heavy designs.

5.3 Parameter set and coding

The geometric parameters and constraints are divided into fixed parameters that are kept constant throughout the entire run and into genetic variables that are optimized.

The fixed parameters and constraints are:

- *total cost of the yacht*
- *wind gust for sizing of mast and rig*
- *surface roughness of hull*
- *stem- and stern-angle*
- *I-P (= gap between mainsail and deck)*
- D_C
- T
- J/I

The genetic variables are:

- | | | | |
|---------------------|---------------------|---------|---------------------|
| ○ L_{WL} / B_{WL} | ○ I | ○ C_P | ○ t_{KR} / C_{KR} |
| ○ B_{WL} / T_C | ○ E | ○ LCB | ○ t_{KT} / C_{KT} |
| ○ α | ○ C_{KR} / L_{WL} | ○ V | |
| ○ β | ○ C_{KT} / C_{KR} | | |

At the start of this research project additional parameters were used to describe the sailplan like aspect ratios of fore and main and roach. It turned out that a variation of these parameters has only a small effect on VMG. This is consistent with the findings in [20]. Therefore the roach is kept constant and reefing supposedly does not change the aspect ratio of a sail.

A negligible effect had also the variation of the side flare in the fore body. Reduced flare reduces the wave drag but it also reduces the sail carrying capacity. The net effect is close to zero.

The values of the variables are represented by binary strings and the 13 strings are concatenated to a chromosome of 53 bits length. The choice of the chromosome length is a trade off between resolution and computing speed. For more details on coding genetic algorithms see [21].

5.4 Merit function

As described in the 1. chapter the merit function is the weighted average of the VMG at two different wind speeds. Figure 6 shows the VMG as a function of wind speed. It seems that the VMGs at 4 kts. and at 44 kts. wind speed are two discernible operating points that describe the yachts performance in light winds and under gale conditions. Also for an increase of the mast length by 2 meters the two operating points still describe the performance well.

The average speed in knots is calculated from

$$VMG_{aver} = \frac{150 + 36 \cdot VMG(44)}{36 + 150 / VMG(4)} \quad (3)$$

which resembles the average speed of a yacht that travels 150 nm in 4 kts. winds and 36 hours in 44 kts. winds.

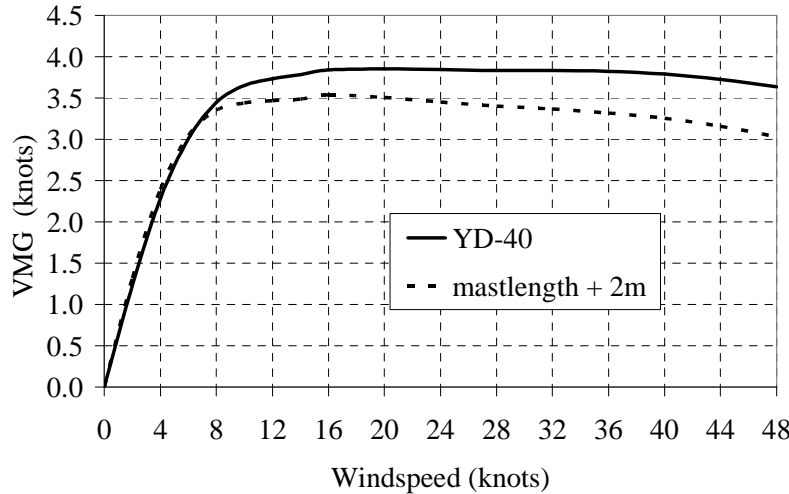


Figure 6. VMG as function of wind speed for YD-40

5.5 Computing process

A start population of 400 independent designs was randomly created. Each following generation is formed using crossover and mutation. The optimization history for 50 generations is shown in figure 7. The computing time on a 3 GHz pentium4 machine was 80 hours. If the new offspring must be discarded because no solution for the

force equilibrium can be found, it is replaced by a randomly generated individual. This is the reason for the difference that still occurs between the maximal and the mean value. It keeps the population divers and avoids premature convergence.

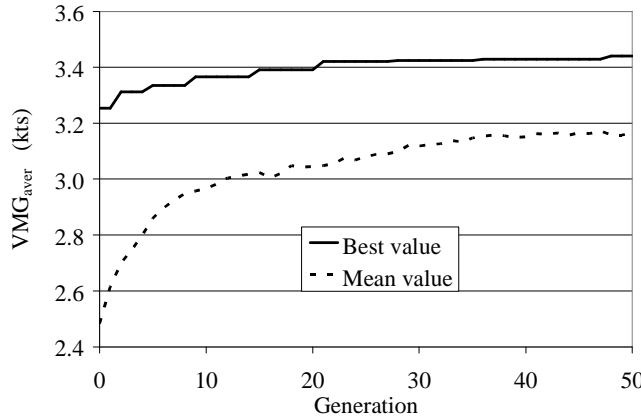


Figure 7. Optimization history

6. RESULTS

6.1 Overall solution space

A two-dimensional plot of the single VMGs at the two wind speeds for all yachts, calculated during the computation of the 50 generations, is shown in figure 8. Each solution is located by its VMG(4) and its VMG(44). It is possible to draw an envelope curve around all points that locates the fastest solutions. All points on the dashed curve are "pareto optimal" in a mathematical sense. An improvement of the VMG at one wind speed can only be achieved at the expense of reducing the VMG at the other one. The optimal average VMG that is marked with an arrow must also be lying on this curve. The cross marks the VMGs of the YD-40 design for comparison. The optimizer has successfully found a large number of designs that are up to 23% faster in VMG_{aver} than the YD-40.

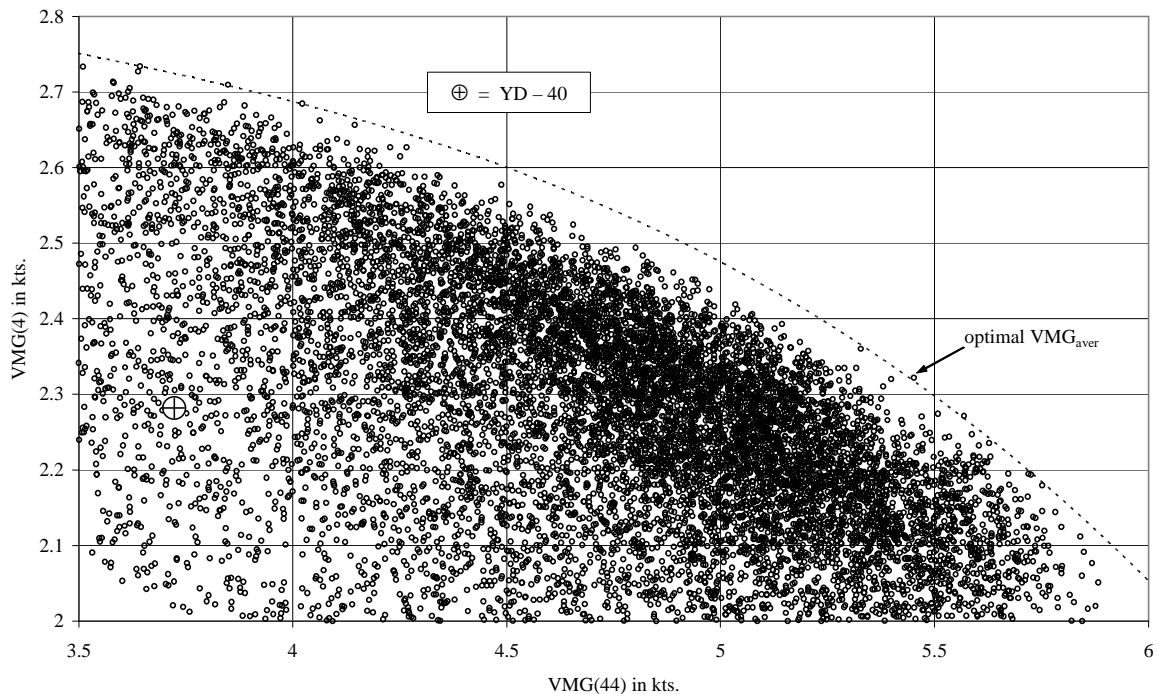


Figure 8. Optimization results

6.2 Optimal parameter sets

The main design parameters of the optimum and two other designs, which stood out, are listed together with the YD-40 data in the following table:

	Optimal average VMG	Optimum at light winds	Light displacement	YD-40
L_{WL} (m)	12.02	10.73	10.59	10.02
B_{WL} (m)	2.62	2.81	3.60	3.17
T_C (m)	1.06	1.01	0.43	0.57
$\nabla \cdot \rho_w$ (kg)	11730	9215	5890	8120
$L_{WL}/\nabla^{1/3}$	5.33	5.16	5.91	5.03
Ballast ratio	59%	48%	17%	40%
Cabin (m^2)	15.3	17.8	34.3	25.0
Beating to windward				
VMG(44)	5.45	3.64	3.68	3.72
VMG(4)	2.32	2.73	2.28	2.28
VMG _{aver}	3.44	3.09	2.77	2.79
Reaching at 12 kts. wind speed, heading 120°				
V (kts)	7.86	8.19	8.45	7.76

An obvious result of the optimization is the advantage of high ballast ratios. The length/displacement ratio shows, that the designs are not heavy; instead the optimizer has tried to create a large but narrow yacht with a long waterline and kept the weight of the canoe body small, as this is the main cost driver. The small size of the cabin area, which is here defined as the water plane area 1.5 m below the highest point of the canoe body, might be a drawback that needs to be considered when choosing a design. The fact that the design was optimized for beating to windward does not imply that the design is slow on other courses. To prove this, the table shows the predicted speed when reaching at an angle of 120° between course and wind direction. The results are favorable.

The lines drawing that can be created from the transformed hull based on the optimal parameter set will eventually decide about the feasibility of the designs.

7. CONCLUSION AND NEXT STEPS

This paper described an efficient tool to create a number of high performance designs in an automated way. The advantage of this computer program consists not only in the saving of time and manpower but also in the chance that the program can create unusual parameter sets the naval architect would normally not consider. Taking the average of the three simulated operating points, an optimized design can be 14% faster than a conventional cruising design as reflected in [1]. Even for a cruising sailor it makes a difference whether a passage takes 17 or 15 days.

In a next step the computing time needs to be reduced. The independent computing of the VMGs at the two different wind speeds lends itself very naturally to parallel computing. This will require rewriting of the source code with the potential of cutting computing time nearly in half. By then one will have a standard tool that can routinely be used in the design process to deliver optimized designs in an automated way. A complete survey of the design space that takes an experienced designer several weeks with today's iterative methods can then be performed unattended by the computer within two days.

8. REFERENCES

1. Larsson, L. & Eliasson, R. E. (1994), *Principles of Yacht Design*, Adlard Coles, London GB.
2. Gerr, D. (2000), *Boat Strength*, International Marine, Camden USA.
3. Oossanen, P. van (1993), "Predicting the Speed of Sailing Yachts", *SNAME Transactions*, **101**, 337-397.

4. www.cyberiad.net/leo.htm
5. Kuhn, J. C., Scragg, C. A. (1993), "Analysis of Lift and Drag on a Surface-Piercing Foil", *The 11th Chesapeake Sailing Yacht Symposium, SNAME SC-2*, 277-288.
6. Keuning, J. A. & Sonnenberg, U.B. (1998), "Approximation of the Hydrodynamic Forces on a Sailing Yacht based on the Delft Systematic Yacht Hull Series", *The international HISWA Symposium on Yacht Design and Yacht Construction*, RINA, pp 99-152.
7. Keuning, J. A. & Katgert, M. (2008), "A Bare Hull Resistance Prediction Method Derived from the Results of the Delft Systematic Yacht Hull Series Extended to Higher Speeds", *Innovation in High Performance Sailing Yachts, Lorient, France*, RINA, pp 13-21.
8. Cebeci, T., Cousteix, J. (1999), *Modelling and Computation of Boundary-Layer Flows*, Springer.
9. Hoerner, S. (1965), *Fluid-Dynamic Drag*, Published by the Author, USA.
10. Binns, J. R., Thompson, R., Brandner, P. A. (2011), "Free-Surface Effects of Variations in Appendage Vertical Volume Distribution: Where Does a Bulb Not See the Free Surface?", *The 20th Chesapeake Sailing Yacht Symposium*, SNAME , pp 71-77.
11. Michel, W. H. (1999), "Sea Spectra Revisited", *Marine Technology*, **36**(4), 211-227.
12. Milgram, J. H. (1978), "Effects of Masts on the Aerodynamics of Sail Sections", *Marine Technology*, **15**(1), 35-42.
13. Lakshminarayana, B. (1964), "Effects of a Chordwise Gap in an Airfoil of Finite Span in a Free Stream", *Journal of the Royal Aeronautical Society*, **68**, 276-280.
14. Hansen, H. (2006), *Enhanced Wind Tunnel Techniques and Aerodynamic Force Models for Yacht Sails*, PhD-thesis University of Auckland, NZ.
15. Drennan, W. M. et al. (2003), "On the wave age dependence of wind stress over pure wind seas", *Journal of Geophysical Research*, **108**(C3), 8062, 10-1 – 10-13.
16. Belcher, S. E. & Hunt, J. C. R. (1998), "Turbulent Flow over Hills and Waves", *Annual Review of Fluid Mechanics*, **30**, 507-538.
17. Motzfeld, H. (1937), "Die turbulente Strömung an welligen Wänden", *Zeitschrift für angewandte Mathematik und Mechanik*, **17**(4), 193-212.
18. Press, W. H. et al. (1992), *Numerical Recipes*, Cambridge University Press, GB.
19. Day, A. H. (1993), "Steps towards an Optimal Yacht Sailplan", *Transactions of RINA*, **135**, 155-173.
20. Day, S. (1995), "The Design of Yacht Sailplans for Maximal Upwind Speed", *The 12th Chesapeake Sailing Yacht Symposium, SNAME SC-2*, 97-116.
21. Goldberg, D. E. (1989), *Genetic Algorithms*, Addison-Wesley, USA.